Peripheral refractive errors in myopic, emmetropic, and hyperopic young subjects

Anne Seidemann and Frank Schaeffel

University Eye Hospital, Section of Neurobiology of the Eye, Calwerstrasse 7/1, 72076 Tübingen, Germany

Antonio Guirao, Noberto Lopez-Gil, and Pablo Artal

Laboratorio de Optica, Departmento de Física, Universidad de Murcia, Campus de Espinardo (Edificio C), 30071 Murcia, Spain

Received January 28, 2002; revised manuscript received July 18, 2002; accepted July 22, 2002

To gain more insight into the relationship between foveal and peripheral refractive errors in humans, spheres, cylinders, and their axes were binocularly measured across the visual field in myopic, emmetropic, and hyperopic groups of young subjects. Both automated infrared photorefraction (the "PowerRefractor"; www.plusoptix.de) and a double-pass technique were used because the PowerRefractor provided extensive data from the central 44 deg of the visual field in a very convenient and fast way. Two-dimensional maps for the average cross cylinders and spherical equivalents, as well as for the axes of the power meridians of the cylinders, were created. A small amount of lower-field myopia was detected with a significant vertical gradient in spherical equivalents. In the central visual field there was little difference among the three refractive groups. The established double-pass technique provided complementary data also from the far periphery. At 45 deg eccentricity the double-pass technique revealed relatively more hyperopic spherical equivalents in myopic subjects than in emmetropic subjects [$\pm 2.73 \pm 2.85$ D relative to the fovea, $p < 0.01$ ($\pm$standard deviation)] and more myopic spherical equivalents in hyperopic subjects (-3.84 ± 2.86 D relative to the fovea, $p < 0.01$). Owing to the pronounced peripheral astigmatism, spherical equivalents (refractions with respect to the plane of the circle of least confusion) became myopic relative to the fovea in all three groups. The finding of general peripheral myopia was unexpected. Its possible roles in foveal refractive development are discussed. © 2002 Optical Society of America

OCIS codes: 170.0170, 330.4460, 330.7310, 330.4300.

1. INTRODUCTION

If scleral growth in human eyes were controlled by image processing in local retinal areas, as in chicks[1,2] and guinea pigs,[3] foveal refractions could scarcely develop independently from the peripheral refractions. To move the position of the retinal plane, scleral tissue must expand or contract in a tangential direction, either by remodeling[4] or by stretching.[5] Expansion of scleral tissue in the periphery of the fovea would most likely also have an effect on the foveal position along the fixation axis, whereas expansion or contraction of the scleral tissue directly underlying the fovea should not have a large effect on its axial position since it would expand the back of the globe mainly in the lateral direction. Therefore the growth of the peripheral sclera is an important variable for emmetropization in the fovea. In eyes with hyperopia in the periphery, more scleral expansion is expected, which should also move the fovea in the myopic direction. Conversely, in eyes that are myopic in the periphery, more foveal hyperopia should develop. Such a pattern of off-axis refractions was indeed found in ametropic adult subjects[6,7] and in children with existing foveal refractive errors.[8] It is striking that the observed peripheral refractive errors were such that they would help to reduce the foveal refractive error. Unfortunately, studies in eyes that had already undergone some period of emmetropization cannot help in deciding whether the peripheral refractive errors are a consequence or a cause of foveal refractive development. A number of studies have described how the optical features of cornea and lens determined the peripheral refractions, but they have not addressed the possible implications for emmetropization (e.g., Refs. 9 and 10). Changes in axial eye growth inevitably produce changes in the shape of the globe and therefore changes in peripheral refractions.

Although there may be interactions between peripheral and foveal refractive development, when they are considered together, causes and consequences of refractive changes cannot be separated. Given the considerable variability among different studies, it is not even clear whether emmetropization occurs at all in the peripheral retina of the human eye. Therefore the following questions are studied in the present paper: (1) Can the pattern of peripheral refractions that was previously observed with a commercial autorefractor in the different refractive groups (Topcon Refractometer Model III[6]; Canon R-1 autorefractor[8]) be confirmed and extended with our refraction techniques (photorefraction and the double-pass technique)? In particular, since the published data were restricted to one horizontal meridian, more-complete two-dimensional retinal refraction maps could provide new input for an answer to the question. (2) Because eccentric photorefraction[11] provides extensive data in a short time, it was used for the first time to mea-

sure sphere, cylinders, and axes in the peripheral visual field. Since it was necessary in the present study to use the double-pass technique to add complementary data for more-peripheral positions, how well does photorefraction agree with the established double-pass technique?[12] Finally, (3) do the observed refractions provide evidence for emmetropization in the periphery (which would mean that refractive errors are also minimized in the periphery), and, if so, does emmetropization minimize peripheral refractive errors for the circle of least confusion or for one of the ends of Sturm's interval?

2. METHODS

A. Photorefractor

The automated eccentric infrared photorefractor, the "PowerRefractor,"[13] determined refractions from the slopes of the brightness distributions in the pupil.[11] The brightness gradients were generated by an array of infrared light-emitting diodes (LEDs, peak emission at 850 nm) positioned below a knife edge in the camera aperture. The PowerRefractor used a six-armed retinoscope with six such arrays to determine the refractions sequentially in the 30-, 90-, and 150-deg pupil meridians.[14] The negative-cylinder convention was used throughout the study (dioptric difference from the least myopic meridian to the most myopic meridian given in negative dioptric values and the spheres given as the refraction in the least myopic meridian). Spherical equivalents (average of the refractions in the least and the most myopic meridian: the refraction of the plane of the circle of least confusion) were studied because they describe the gross image defocus. In addition, the cross cylinders (half of the total astigmatism) were evaluated (see Figs. 2 and 3 below; note that in Figs. 2 and 3, the refractions are plotted relative to the foveal refractions, which makes it possible that averages of the negative cylinders can be positive in a few cases). The PowerRefractor recorded data peripherally only up to ~25 deg from the fixation axis, depending on pupil size, because its image-processing algorithms required that the first Purkinje image of the light source, in this case of the LED array, appear in the pupillary area. The PowerRefractor also automatically located the first Purkinje image and determined the position of the pupil axis by evaluating its centration in the pupil. The pupil axis is a few degrees temporal from the fixation axis, separated by the angle "kappa" (which was measured as 3.9 ± 2.7 deg in young subjects[15]).

B. Double-Pass Method

The double-pass apparatus[16,17] was similar to others previously applied for measurements in the peripheral visual field.[18–20] It permitted recording of double-pass images that kept information on the odd aberrations.[21] Briefly, the technique worked as follows: Light emerging from a He–Ne laser source (wavelength 543 nm) was expanded and collimated and reached the eye after reflection by a beam splitter. An artificial pupil was projected onto the subject's pupil, acting as an aperture stop. The point source formed an aberrated image on the retina (first pass). Part of the light was reflected from the fundus and captured by a camera when leaving the eye (second pass). Double-pass images (4-s exposure) were recorded with a scientific-grade cooled CCD camera (Compuscope CCD 800) and digitized with 256×256 pixel size (corresponding to a field of view of 80 arc min) and a resolution of 12 bits/pixel.

Peripheral defocus and astigmatism were determined by using equal 1.5-mm-diameter pupils in both passes. Focus positions were scanned with a precision of 0.1 diopter (D) to find the double-pass images that correspond to the extremes of the Sturm interval: sagittal and tangential foci, with the least-confusion circles between them. To validate the estimated value of astigmatism, an additional double-pass image was recorded, with the astigmatism corrected by placing the appropriate cylindrical lens for the sagittal focus. If this image was not elongated and was more compact than the image corresponding to the least-confusion circle, it was concluded that astigmatism was appropriately corrected and that the correct value was measured. Additional details on this procedure to estimate peripheral refractions can be found in Ref. 19.

C. Measurement Procedures

The PowerRefractor recorded defocus (sphere), astigmatism (cylinder), and axes from a stationary position at 1 m distance (±5%) from the subject. Refractions were determined at the various angles by asking the subjects to read letters of 1 cm height (0.57-deg field) that were attached to a large plane cardboard plate at 5.7, 8.3, 14.3, and 21.8 deg eccentricity with respect to the video camera of the PowerRefractor, with a total of 45 individual locations. Accommodation was controlled by the target distance. The subjects used a chin rest but no bite bar. All subjects with refractive errors were measured with their spectacle corrections. In these cases, they were asked to keep head orientation straight and to fixate the peripheral targets through the periphery of their spectacles. This ensured that no artificial astigmatism was introduced in the direction of measurement by tilting the spectacle lenses. A small offset might have been introduced for the most peripheral fixation targets, since the target plane was flat and the distance increased slightly to the periphery (~0.07 D more distant at 22 deg). No correction was made for potential accommodation changes when the subjects looked through the periphery of their spectacles. The luminance of the targets was ~50 cd/m^2, and the illuminance in the room was 200 lux, provided by incandescent light.

In the double-pass technique, subjects used a chin rest and fixated a green LED viewed through a mirror and located at optical infinity, which was positioned at different locations within the visual field (15, 20, 30, 40, and 45 deg in the temporal horizontal meridian). During these measurements, the subjects did not wear their glasses and were therefore not forced to keep head orientation straight.

To facilitate the comparisons of the peripheral refraction patterns in the three groups (see Figs. 2–5 below), the foveal refractive errors were subtracted from each peripheral refractive error. As a result, the refractions at the fovea are plotted as zero. In Figs. 2 and 3 below, the absolute values of the individual cross-cylinder values

were averaged without consideration of their angles, because these figures show how much absolute astigmatism was present at each angular position. It was not intended to average the three-dimensional refraction data in the way the power of combined astigmatic lenses is calculated, since astigmatism of different subjects could cancel out so that the averages would no longer represent the average amount of total astigmatism. Spherical equivalents can be arithmetically averaged.[8] On the other hand, this is not possible for the axes of astigmatism of different subjects (Fig. 4 below). The following procedure (described by Oechsner and Kusel[22]) was used. From the measurements of n spheres s_i (negative), cylinders c_i, and axes ϕ_i, the following parameters were calculated [Eqs. (1)–(3)]:

$$s_{e,i} = s_i + c_i/2, \tag{1}$$

$$c_{1,i} = (-c_i/2)\cos(2*\phi_i), \tag{2}$$

$$c_{2,i} = (-c_i/2)\sin(2*\phi_i). \tag{3}$$

Since these parameters are mathematically independent, their averages could be determined and backconverted into the averages of spheres, cylinders, and axes by using Eqs. (4)–(6):

$$s_{\text{ave}} = s_e + \sqrt{(c_1{}^2 + c_2{}^2)}, \tag{4}$$

$$c_{\text{ave}} = -2\sqrt{c_1{}^2 + c_2{}^2)}, \tag{5}$$

$$\phi_{\text{ave}} = 0.5 \arctan(c_2/c_1), \tag{6}$$

The calculations were performed by using a small computer program, kindly provided by R. Kusel, Hamburg, Germany. Results were verified in random cases by using the procedure described by Harris.[23] Figure 4 below shows the average astigmatism, as determined by this procedure (different from that of Figs. 1 and 2). Its magnitude is denoted by the length of the lines and the angle of the meridian with the highest power by their orientations.

D. Comparison of the Two Refraction Techniques

In six subjects, measurements were performed with both the double-pass technique and the PowerRefractor under the same visual angles and under the same viewing conditions. For this purpose, the PowerRefractor was taken to Murcia, Spain. Examples of spheres and cylinders measured with both techniques in two subjects are shown in Fig. 1A. Figure 1B compares refraction data from six other subjects, measured at 15, 20, and 25 deg from the fixation axis. Both techniques compared favorably [PowerRefractor (y) versus the double-pass technique (x). Spheres: $y = 0.21 + 1.02x$, $R = 0.848$, $n = 42$ individual measurements; astigmatism: $y = 0.29 + 1.09x$, $R = 0.713$, $n = 37$ measurements, significant correlations ($p < 0.001$) in both cases]. There was no significant dioptric offset or differences of the slopes of the regressions from 1 (unpaired t-tests) despite the fact that they used different wavelengths since the PowerRefractor was previously calibrated to match subjective refractions in white light.[13] The average absolute difference between the spheres measured with both techniques was 0.78 D and between the cylinders was 0.85 D ($n = 42$ measurements). The reliability of measurement for the angles of astigmatism could not be studied because they were all close to 90 deg at the peripheral positions. That

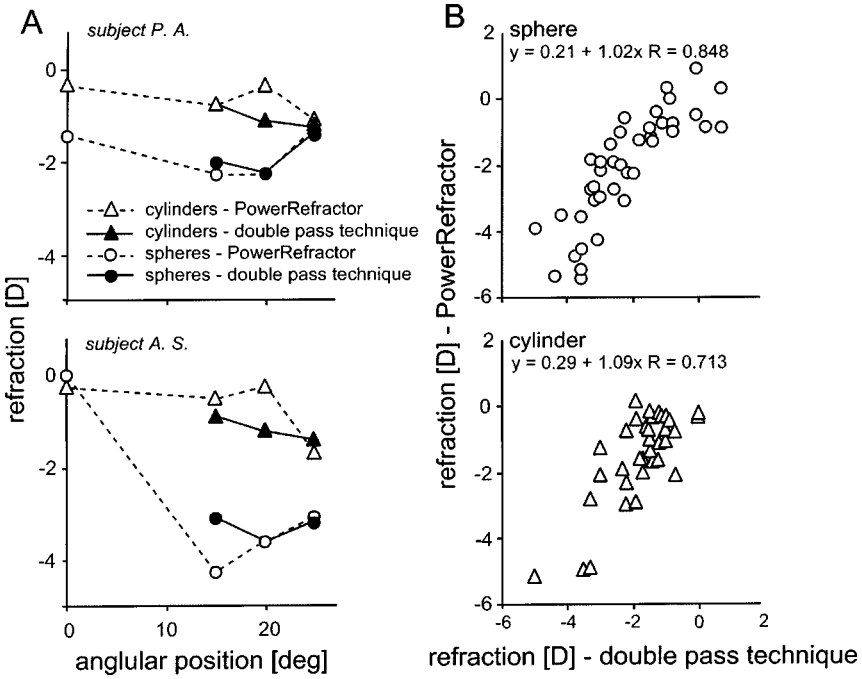

Fig. 1. Comparison of measurements with the double-pass technique and with photorefraction (the PowerRefractor). A, Spheres and cylinders recorded at four angular positions in two subjects. Open symbols, PowerRefractor; solid symbols, double-pass technique [no data with the double-pass technique at the fixation axis (0 deg)]. B, Measurements of spheres and cylinders in six subjects and at 15, 20, and 25 deg in the temporal retina (nasal visual field). The average absolute differences between the double-pass technique and the PowerRefractor were 0.78 D (spheres) and 0.85 D (cylinders). Angles of astigmatism were not evaluated since they were all close to 90 deg with both techniques.

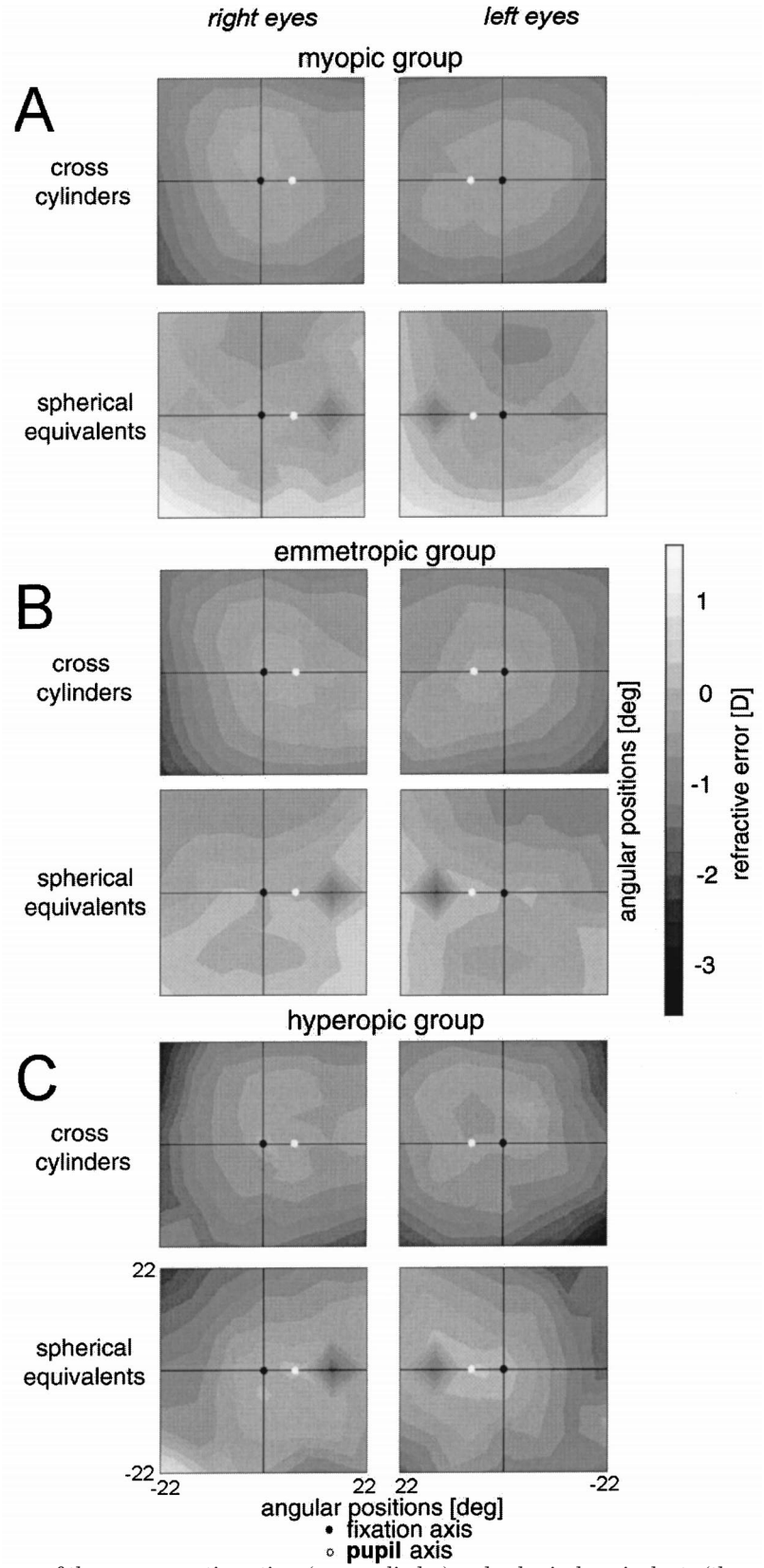

Fig. 2. Gray-level-coded maps of the average astigmatism (cross cylinder) and spherical equivalents (the refraction at the plane of the circle of the least confusion) in the central 44 deg of both eyes of the myopic (A, n 18), emmetropic (B, $n = 8$), and hyperopic groups (C, $n = 5$). Coordinates are retinal coordinates, as seen from the vitreal side; the origin of each plot represents the fovea (black dot). The nasal retina is oriented toward the midline, as can be seen from the position of the optic disk, which shows up in the map of the spherical equivalents as an area of higher myopia. To facilitate intergroup comparisons, the foveal spherical equivalents and the cross cylinder were subtracted from the respective values measured in the periphery. For details on the averaging procedures for the refractions, and on the measurement of the pupil axis, see Section 2. Data in Figs. 2–4 originate from the PowerRefractor.

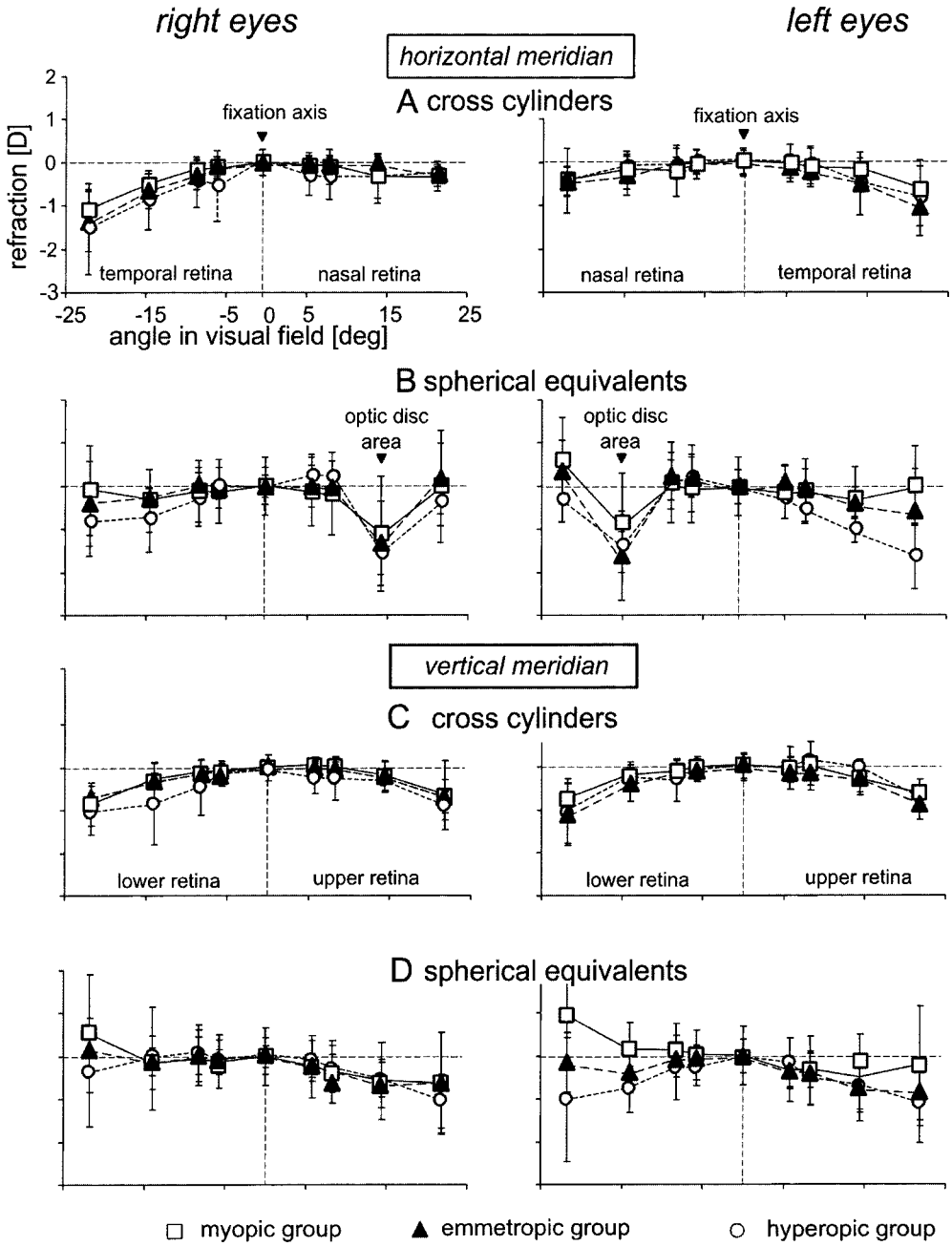

Fig. 3. Average cross cylinders (A, C) and spherical equivalents (B, D) along the horizontal (A, B) and vertical (C, D) meridians of the retina, plotted with respect to the fovea. Open squares, myopes; solid triangles, emmetropes; open circles, hyperopes. Error bars denote standard deviations. Note the asymmetry in the cross cylinders (A), the location of the optic disk in the nasal retina (B), the symmetrical increase of astigmatism in the vertical meridian toward the periphery (C), and the slight increase of myopia from the lower to the upper retina (D) (corresponding to the lower visual field). For details on the averaging procedures, see Section 2.

the PowerRefractor records the axis of astigmatism correctly if the refractions occur centrally has previously been shown.[13]

E. Subjects

Thirty-one young adult subjects (ages ranging from 21 to 33 yr.) were recruited from the University of Tübingen by posted announcements. Eight subjects were emmetropic (foveal spherical refraction between -0.75 and $+1.0$ D, average refraction -0.17 ± 0.49 D), 18 were myopic (< -0.75 D, average refraction -3.06 ± 1.62 D), and 5 were hyperopic (>1 D, average refraction $+4.50 \pm 2.21$ D). To compare off-axis refractions in different refractive groups by the double-pass technique, 11 emmetropic (average refraction 0.11 ± 0.35 D), 9 myopic (average refraction -4.75 ± 1.90 D), and 5 hyperopic (average refraction $+2.42 \pm 1.16$ D) subjects (ages ranging from 21 to 28 yr.) were recruited from the University of Murcia. All subjects were free of any known ocular pathology and had normal corrected visual acuity (20/20 or better). They entered the study after the goals and procedures were explained and their consent was obtained. The pro-

cedures adhered to the declaration of Helsinki for research involving human subjects.

3. RESULTS

A. Maps of Spherical and Cylindrical Refractive Errors for the Myopic, Emmetropic, and Hyperopic Subjects

A comparison of astigmatism (cross cylinders) and spherical equivalents for the three groups in the central ±22 deg of the visual field is shown in Figs 2A–2C. All gray-level coded refraction maps refer to retinal coordinates, as seen from the vitreal side. The two eyes of the subjects were largely mirror images of each other. In the plots of the average absolute cross cylinders, it can be seen that in emmetropes, there was a central area with less than 1 D of astigmatism that extended to ~10 deg peripherally into the nasal retina (corresponding to the upper temporal visual field). The range with low astigmatism was largest in the emmetropic group, less in the myopic group, and smallest in the hyperopic group. Beyond 10 deg off axis, astigmatism increased rapidly. The highest amount of astigmatism was observed in the hyperopic group. In the plots of the spherical equivalents, the optic disk in the nasal retina showed up as a region with, on average, ~1 D more myopia. The spherical equivalent in the periphery (22 deg temporal from the fovea) in the hyperopic subjects (-1.24 ± 1.08 D) was relatively more myopic than in the myopic subjects (-0.039 ± 1.38 D, $p < 0.01$) if the two eyes were pooled. Differences from the emmetropic group did not achieve significance.

The distribution of astigmatism and spherical equiva-

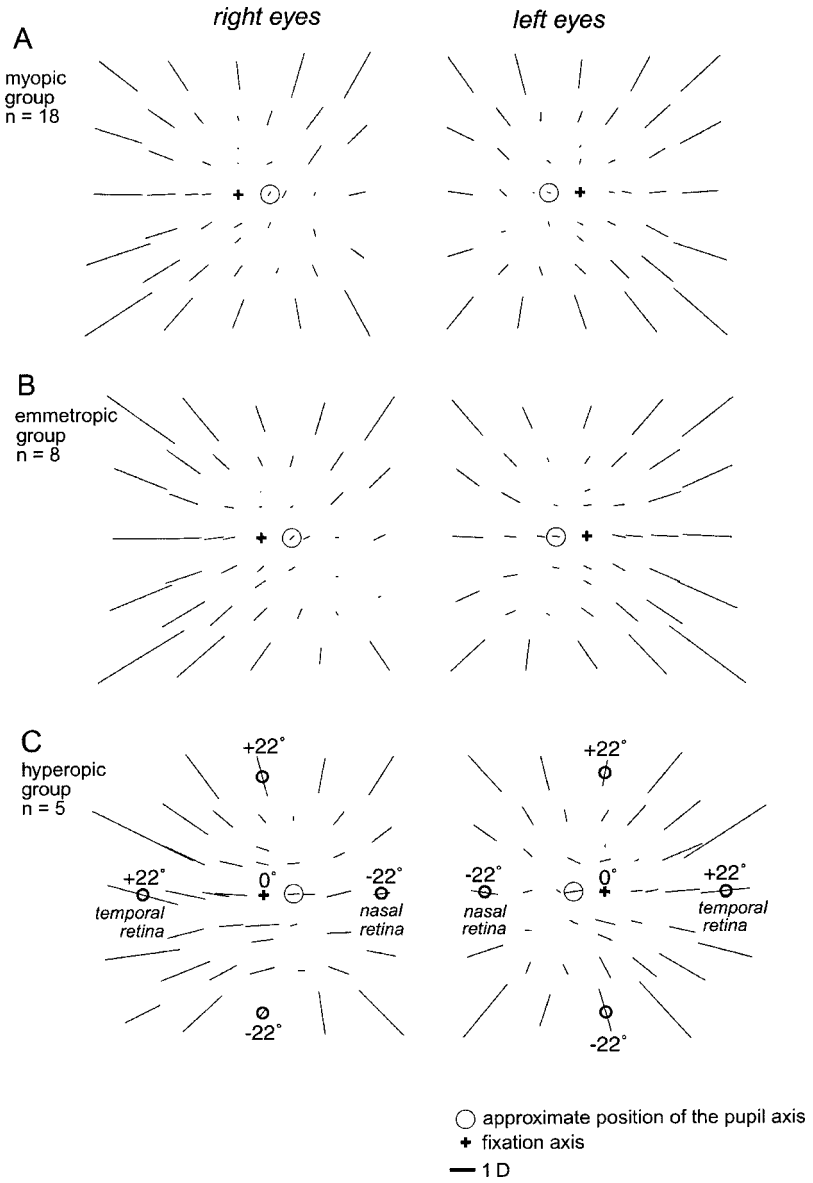

Fig. 4. Orientation and magnitude of the average astigmatism in the myopic (A), emmetropic (B) and hyperopic (C) group. The orientation of the meridians of highest power are denoted by the orientations of the lines. Note that the power axes are approximately radially aligned, with their intersections closer to the pupil axes (circles) than to the fovea (crosses). The magnitude of the cylinders is indicated by the length of the individual lines (see dioptric scale at bottom). Refractions were sampled at 5.7, 8.3, 14.3, and 21.8 deg in the peripheral visual field. For details on the averaging procedures, see Section 2.

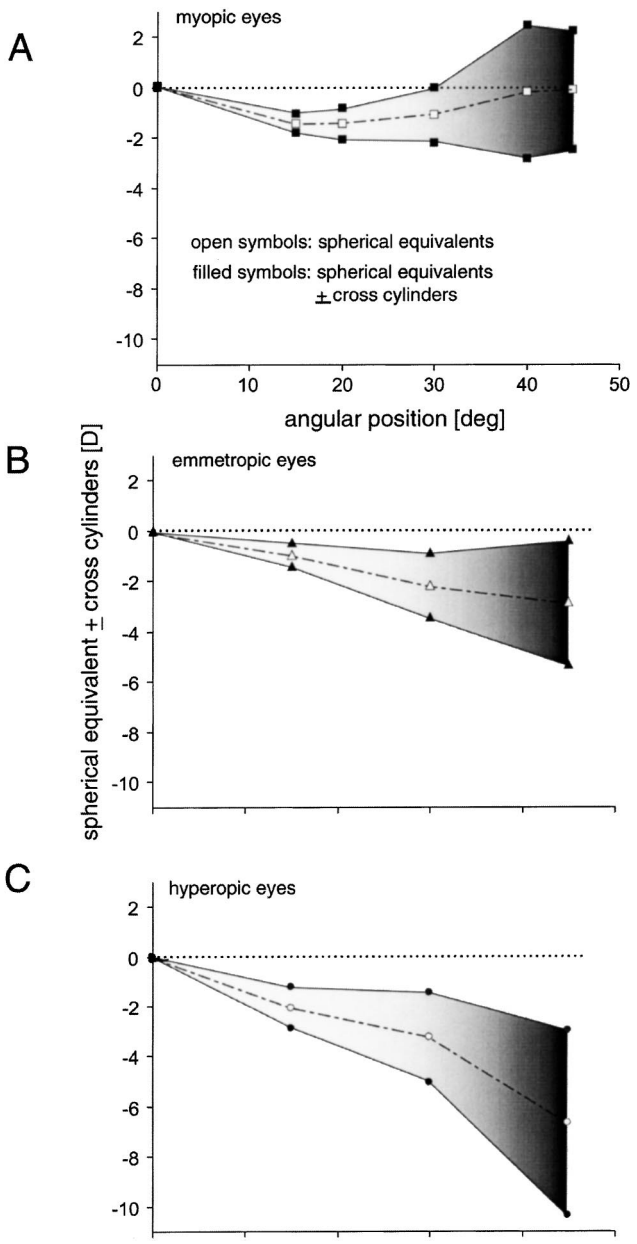

Fig. 5. Peripheral refractive errors, relative to the foveal refractive error, in the myopic (A), emmetropic (B), and hyperopic groups (C). The dashed lines with open symbols are the spherical equivalents, and the top and bottom lines with solid symbols represent the extremes of the Sturm interval and denote the full amplitude of astigmatism. Data shown originate from measurements with the double-pass technique.

lents across the visual field are plotted separately in Fig. 3. No significant differences can be seen among the three groups, either in the horizontal meridians (Figs. 3A and 3B) or in the vertical meridians (Figs. 3C and 3D). There was some asymmetry with respect to the fovea in the astigmatism in the horizontal meridians (3B) but not in the vertical meridians (3D). The spherical equivalents were more myopic in the upper retina (corresponding to the lower visual field) than in the lower retina. The asymmetry showed up in a linear regression analysis (regression lines are not shown in Fig. 3D) through the spherical equivalents along the vertical meridian. Right eyes: hyperopes, refraction (y) = -0.016*angular position(x) $-$ 0.27, $R = 0.633$, $p < 0.05$; myopes; $y = -0.023*x - 0.17$, $R = 0.902$, $p < 0.01$; emmetropes, $y = -0.018*x - 0.20$, $R = 0.899$, $p < 0.01$. Left eyes: $y = -0.002*x - 0.54$, $R = 0.057$, n.s.; myopes, $y = -0.027*x - 0.02$, $R = 0.862$, $p < 0.01$; emmetropes, $y = -0.016*x - 0.33$, $R = 0.732$, $p < 0.01$. The significances were variable in each individual case but became high if all cases were pooled ($p < 0.001$), and there is no doubt that the lower visual field was more myopic than the upper field with a gradient of -0.0169 ± 0.0085 D per angular degree (~0.17 D for 10 deg).

B. Orientation of the Power Meridians

Since the PowerRefractor also provided the axis of astigmatism at each measured angular position in the visual field, the distribution of axes of the power meridians (orientations of the meridians with highest refractive power) could be displayed in a map (Figs. 4A–4C). This map is a representative illustration of the peripheral astigmatism in the human eye. Power meridians were approximately radially oriented, intersecting close to the pupil axis of the eye. The lengths of the bars in Fig. 4 denote the magnitude of the astigmatism. Astigmatism increased to ~2 D in the nasal retina at 22 deg but to only ~1 D in the temporal retina (emmetropic subjects, Fig. 4B). In the myopic and emmetropic groups, astigmatism reached a minimum along a line extending approximately from the pupil axis at 45 deg to down into the temporal retina (Figs. 4A and 4B). In the hyperopic group (Fig. 4C), astigmatism was generally higher and the power meridians were preferentially oriented in the horizontal direction.

C. Measurements with the Double-Pass Technique

Because the photorefraction technique provided data only up to ~25 deg peripherally, complementary peripheral refractions were obtained with the double-pass technique. Measurements were confined to the nasal visual field (temporal retina). The spherical equivalents of all three groups (Fig. 5, open symbols) became myopic in the periphery relative to the fovea but also differed significantly from each other at 45 deg eccentricity: myopes, -0.12 ± 2.27 D, $n = 9$; emmetropes, -2.85 ± 1.72 D, $n = 11$; hyperopes, -6.695 ± 2.29 D, $n = 5$; myopes versus emmetropes; $p < 0.01$; hyperopes versus emmetropes; $p < 0.01$. There were also significant differences among the three groups in astigmatism. At 45 deg temporal, myopes had -4.68 ± 2.14 D astigmatism, emmetropes had -4.94 ± 1.27 D (n.s. versus myopes), and hyperopes had -7.41 ± 2.01 D ($p < 0.05$ versus emmetropes).

When the spherical equivalent is regarded as a measure of the gross image defocus, all groups became myopic in the periphery, relative to the fovea. Only the spherical refractive error (the least myopic meridian in the negative cylinder convention), became relatively more hyperopic in the myopic group beyond 30 deg off axis (Fig. 5A), and, in this group at 45 deg, the spherical equivalent returned to the same refraction as in the fovea.

4. DISCUSSION

We have confirmed previous findings[6–8] that myopic eyes are relatively more hyperopic in the periphery relative to the fovea than are hyperopic eyes. In addition, in our sample, all groups had myopic spherical equivalents in the periphery. Only at 40 deg off axis and higher did eyes with foveal myopia return to the same spherical equivalents as in the fovea (Fig. 5A). Furthermore, we found more myopia in the lower than in the upper visual field, which may be linked to the ramp retinas observed in some animals.[24,25]

A. Comparison with Other Studies on Peripheral Refractions

The first studies on peripheral refraction appeared in 1932 (Ref. 26) and described a nasal–temporal asymmetry that was also observed in the present study (Fig. 3). Millodot[6] was the first to compare subjects with different foveal refractive errors. He found that hyperopes were ~1.5 D more myopic 20 deg temporal from the fovea than were myopes. The result of the present study is similar. A difference from Millodot's data is that in his study, myopes had ~1 D more hyperopic spherical equivalents at 45 deg (solid symbols in Fig. 6A), whereas all refractive groups had myopic spherical equivalents in our sample (open symbols in Fig. 6A). Mutti *et al.*[8] measured peripheral refractions at 30 deg in 827 children and concluded that "relative peripheral hyperopia was associated with myopic ocular component characteristics" (p. 1022). They attributed this to the fact that the shape of the globe becomes distorted as a result of its restriction of equatorial expansion, but they do not give detailed predictions on the eye shapes. The difference in peripheral refractions in emmetropia and myopia described by Millodot[6] and Mutti *et al.*[8] was confirmed by Love *et al.*[7] and by data of the present study.

We measured higher amounts of astigmatism than Millodot did,[6] in particular in the hyperopic group (−7.4 D versus ~4 D at 45 deg, Fig. 6B). This could be due to different techniques of measurement (double-pass technique versus Topcon Refractometer Model III) but also to population differences. However, others have also claimed more astigmatism: Lotmar[27] calculated 5.5 D at 45 deg in a model eye but measured only ~4 D at 45 deg in real eyes.[28] By using the double-pass methods, Williams *et al.*[29] found that astigmatism in the periphery (45 deg) ranged from 4 to 6 D in different subjects. These data are similar to the data in the emmetropic group in the present study. It is clear that the particularly high amounts of astigmatism in our subjects contributed to the myopia in terms of spherical equivalents.

In line with a previous observation by Jennings and Charman,[30] our data suggest that the eyes' astigmatism is apparently not at a minimum at the fovea but rather in the nasal retina (temporal visual field). Dunne *et al.*[31] located a position with minimal astigmatism 8.8 ± 7.0 deg away from the fixation axis in the nasal retina. This angle is larger than kappa (which was measured as

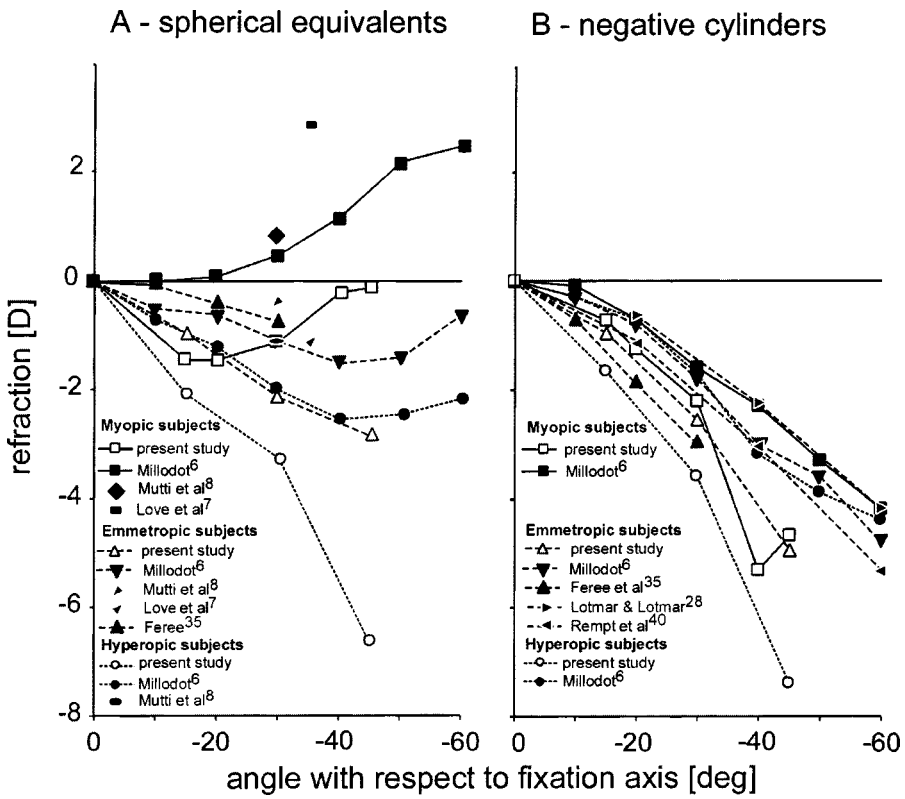

Fig. 6. Comparisons of the spherical equivalents and the negative cylinders measured in this study with published data (sources are denoted in the legends). A, For comparison, all published refractions were converted into spherical equivalents. In particular, in the hyperopic group, more-myopic spherical equivalents were measured in the present study than in previous studies. B, Astigmatism was higher in the subjects of this study than in previous studies, except perhaps for the sample of Feree *et al.*[35] The observed higher astigmatism could account in part for the more-myopic spherical equivalents.

3.9 ± 2.7 deg in young subjects[15]) but even larger than alpha (5.0 ± 1.2 deg,[31] the angular distance between the fixation and the optical axis).

B. Do the Myopic Spherical Equivalents Limit Peripheral Visual Acuity?

Jennings and Charman[30] and Navarro *et al.*[18] measured the peripheral optical quality of the eye with a double-pass technique and found that it is only slightly degraded over the central 25 deg. They concluded that, even at higher eccentricities, the optics were not the limiting factor. Williams *et al.*[29] performed an analysis on the relationship between off-axis optical quality and retinal sampling for various eccentricities. Only for the very central fovea did they find the optics exactly matched to sampling density. For the remaining retina, the optics provided higher spatial resolution than did photoreceptor sampling. However, correcting peripheral refractive error was found to increase some aspects of visual performance in the periphery.[19] On the other hand, behavioral studies show that at 20 deg peripherally, both detection acuity and resolution are largely insensitive to defocus over a dioptric range of ~4 D.[32]

At 30 deg, visual acuity of the human eye is reduced to ~10% of the average foveal acuity of 60 cycles per degree (c/deg), and at 45 deg, it is reduced to only 4%.[33] Even for a visual acuity of 2.4 c/deg (4%), the optical depth of focus is only 2 D or less, as estimated from the modulation transfer function of a diffraction-limited human eye.[34] At 2.4 c/deg and a pupil size of 4 mm, the modulation transfer function approaches zero for ~2 D of defocus. Therefore the relative peripheral myopia exceeds the calculated depth of focus only in the hyperopic subjects.

C. Peripheral Myopia: an Artifact of Mechanical Forces during Eye Rotations or Accommodation?

Ferree *et al.*[35] noticed that peripheral myopia is induced in a short time if the measurement instrument is fixed and the eye moves instead of having the subjects turn their heads or having the instrument rotate. Because this artifact could potentially account for some of the myopic refractions in the periphery, the double-pass technique was used to compare refraction with either the eye rotated or the head rotated. Data are given in Table 1.

There is no doubt that there is a trend toward more myopia if the eyes are voluntarily turned by 40 deg (with three subjects, on average by 0.70 ± 0.36 D). However, the effect is small compared with the measured myopia. Furthermore, in the original measurements with the double-pass technique shown in Fig. 5, it was not necessary to force the subjects to keep their heads straight and to turn their eyes. Therefore it can be excluded that the peripheral myopia shown in Fig. 5 results from the measurement artifact identified by Ferree *et al.*[35] Accommodation was controlled by the fixation distance in the PowerRefractor measurements (at 22 deg peripheral fixation only 7 cm more than centrally, with the plate at 1 m) and by a green LED, optically placed at infinity, in the measurements with the double-pass technique.

Table 1. Difference between Refractions without and with Eye Torsion As Measured with the Double-Pass Technique[a]

Subject	Difference in Sphere (D)	Difference in Cylinder (D)
Eccentricity 20 deg temporal		
PA	0.2 ± 0.2	−0.2 ± 0.1
NL	−1 ± 0.5	0.2 ± 0.1
AG	0.2 ± 0.2	−0.5 ± 0.3
Eccentricity 40 deg temporal		
PA	−0.3 ± 0.3	−0.3 ± 0.3
NL	−1 ± 0.5	0.1 ± 0.3
AG	−0.8 ± 0.7	−3 ± 1

[a] More-negative values indicate more myopia or higher cylinder values with torsion compared with the refractions measured with the eyes straight and the instrument turned. Errors are standard deviations from six measurements in each case.

D. Lower-Field Myopia in Humans?

We found a significant increase in myopia in the lower visual field (upper retina). The gradient was shallow (0.17 D per 10 deg), but it is possible that it relates to the lower-field myopia that is known from a number of animals[36–38] but has not yet been described in humans. In the animals, lower-field myopia is interpreted as an "adaptation to keep the ground in focus" (Ref. 36, p. 653). It is not certain whether the small gradient has adaptive value in humans or is a rudimentary feature of the evolution of the eye. Its presence, however, could be compatible with the idea of emmetropization in the periphery of the visual field.

E. Peripheral Emmetropization for the Least Myopic Meridian, the Spherical Equivalent, or the Most Myopic Meridian?

Given the large amounts of astigmatism in the periphery of the visual field, there are three options regarding where the set point of emmetropization could be located: either at one of the ends of Sturm's interval or at the plane of the circle of least confusion. Emmetropization to the plane of the spherical equivalents appears to be the best solution, since this would probably provide the best possible image. Unexpectedly, the data of the current study suggest that the least myopic meridian was closest to emmetropia (Fig. 5) and that the spherical equivalents were all myopic relative to the fovea. It is possible that the peripheral myopia emerges during genetically preprogrammed eye growth without further visual feedback control or that the periphery emmetropizes for a closer viewing distance (i.e., the average viewing distance over the day). It could even be that myopia in the periphery is a trick of nature to produce a constant inhibitory signal to prevent too much eye growth. It has recently been shown that imposed myopic defocus is normally very potent in inhibiting eye growth in animal models: Positive lenses block myopia that has been induced by negative

lenses even if the positive lenses are worn for only one fifth of the time.[39] Since myopia occurs in human eyes despite intermittent periods of myopic defocus that are most likely experienced over the course of the day, its presence could indicate that the necessity to continuously restrain eye growth is a "weak point" of the emmetropizing system.

Studies on emmetropization in the presence of astigmatic defocus in animal models are inconsistent. On the basis of experiments in monkeys, Smith *et al.*[41] concluded that imposed "astigmatism interferes with normal emmetropization" (p. 336), causing generally more-hyperopic spherical equivalents. Similarly, it was found in chickens that wearing of lenses with spherical equivalents at zero power but with 10 D of total astigmatism produces hyperopia.[42] On the other hand, Schmid and Wildsoet[43] concluded, on the basis of experiments with astigmatic lenses, that eyes of chickens emmetropized to the most myopic meridian.

Schematic models of expansion of the globe in ametropia predict the differences in the peripheral refractions between myopic, emmetropic, and hyperopic subjects. If the globe elongates either elliptically or selectively in the equatorial region, the observed differences in refraction patterns emerge.[8] However, the models do not predict as much peripheral myopia as was measured in the present study. Only if off-axis astigmatism is taken into account do the models provide myopic spherical equivalents similar to the ones measured here.

ACKNOWLEDGMENTS

This study was supported by the German Academic Exchange Service grant Acciones Integradas HA97-0115 to Pablo Artal and Frank Schaeffel, the Max Planck Award to Frank Schaeffel, and the Spain-DGES grant PB97-1056 to Pablo Artal. A preliminary description of some of the data was previously presented.[44]

Send all correspondence to Frank Schaeffel, University Eye Hospital, Section of Neurobiology of the Eye, Calwerstrasse 7/1, 72076 Tübingen, Germany. Phone, 49-7071-2980739; fax, 49-7071-295196; e-mail, frank.schaeffel@uni-tuebingen.de.

REFERENCES

1. J. Wallman, M. D. Gottlieb, V. Rajaram, and L. A. Fugate-Wentzek, "Local retinal regions control local eye growth and myopia," Science **237**, 73–77 (1987).
2. S. Diether and F. Schaeffel, "Local defocus and local eye growth in chicks with normal accommodation," Vision Res. **37**, 659–668 (1997).
3. S. McFadden, "Partial occlusion produces local form deprivation myopia in the guinea pig eye," Invest. Ophthalmol. Visual Sci. Suppl. **43**, #189 (ARVO abstract 2002).
4. N. A. McBrien, P. Lawlor, and A. Gentle, "Scleral remodelling during the development of and recovery from axial myopia in tree shrew," Invest. Ophthalmol. Visual Sci. **41**, 3713–3719 (2000).
5. J. T. Siegwart and T. T. Norton, "Regulation of the mechanical properties of tree shrew sclera by the visual environment," Vision Res. **39**, 387–407 (1999).
6. M. Millodot, "Effect of ametropia on peripheral refraction," Am. J. Optom. Physiol. Opt. **58**, 691–695 (1981).
7. J. Love, B. Gilmartin, and M. C. M. Dunne, "Relative peripheral refractive error in adult myopia and emmetropia," Invest. Ophthalmol. Visual Sci. Suppl. **41**, #1592 (ARVO abstract 2000).
8. D. O. Mutti, R. I. Sholtz, N. E. Friedman, and K. Zadnik, "Peripheral refraction and ocular shape in children," Invest. Ophthalmol. Visual Sci. **41**, 1022–1030 (2000).
9. M. C. Dunne, D. A. Barnes, and R. A. Clement, "A model for retinal shape changes in ametropia," Ophthalmic Physiol. Opt. **7**, 159–160 (1987).
10. M. C. Dunne and D. A. Barnes, "Modelling oblique astigmatism in eyes with known peripheral refraction and optical dimensions," Ophthalmic Physiol. Opt. **10**, 46–48 (1990).
11. F. Schaeffel, H. Wilhelm, and E. Zrenner, "Inter-individual variability in the dynamics of natural accommodation in humans: relation to age and refractive error," J. Physiol. (London) **461**, 301–320 (1993).
12. P. Artal, S. Marcos, R. Navarro, and D. R. Williams, "Odd aberrations and double pass measurements of retinal image quality," J. Opt. Soc. Am. A **12**, 195–201 (1995).
13. M. Choi, S. Weiss, F. Schaeffel, A. Seidemann, H. C. Howland, B. Wilhelm, and H. Wilhelm, "Laboratory, clinical and kindergarten test of a new infrared photorefractor (PowerRefractor)," Optom. Vision Sci. **77**, 537–548 (2000).
14. F. Gekeler, F. Schaeffel, H. C. Howland, and J. Wattam-Bell, "Measurement of astigmatism by automated infrared photorefraction," Optom. Vision Sci. **74**, 472–482 (1997).
15. F. Schaeffel, "Kappa and Hirschberg ratio measured with an automated video gaze tracker," Optom. Vision Sci. **79**, 329–334 (2002).
16. J. Santamaría, P. Artal, and J. Bescós, "Determination of the point-spread function of the human eye using a hybrid optical-digital method," J. Opt. Soc. Am. A **4**, 1109–1114 (1987).
17. A. Guirao, C. Gonzales, M. Redondo, E. Geraghty, S. Norrby, and P. Artal, "Average optical performance of the human eye as a function of age in a normal population," Invest. Ophthalmol. Visual Sci. **40**, 203–213 (1999).
18. R. Navarro, P. Artal, and D. R. Williams, "Modulation transfer of the human eye as a function of eccentricity," J. Opt. Soc. Am. A **10**, 201–212 (1993).
19. P. Artal, A. M. Derrington, and E. Colombo, "Refraction, aliasing, and the absence of motion reversals in peripheral vision," Vision Res. **35**, 939–947 (1995).
20. A. Guirao and P. Artal, "Off-axis monochromatic aberrations estimated from double-pass measurements in the human eye," Vision Res. **39**, 207–217 (1999).
21. P. Artal, I. Iglesias, N. Lopez-Gil, and D. G. Green, "Double-pass measurements of the retinal image quality with unequal entrance and exit pupils sizes and the reversibility of the eye's optical system," J. Opt. Soc. Am. A **12**, 2358–2366 (1995).
22. U. Oechsner and R. Kusel, "Multimeridional refraction: dependence of the measurement accuracy on the number of meridians refracted," Optom. Vision Sci. **73**, 425–433 (1997).
23. W. F. Harris, "Algebra of sphero-cylinders and refractive errors, and their means, variance, and standard deviation," Am. J. Optom. Physiol. Opt. **65**, 794–802 (1988).
24. G. L. Walls, *The Vertebrate Eye and Its Adaptive Radiation* (Cranebrook Institute of Science, Bloomfield Hills, Mich., 1942).
25. J. G. Sivak, "An evaluation of the 'ramp' retina of the horse eye," Vision Res. **15**, 1353–1356 (1975).
26. C. E. Ferree, G. Rand, and C. Hardy, "Refractive asymmetry in the temporal and nasal halves of the visual field," Am. J. Ophthalmol. **15**, 513–522 (1932).
27. W. Lotmar, "Theoretical eye model with aspherics," J. Opt. Soc. Am. **61**, 1522–1529 (1971).
28. W. Lotmar and T. Lotmar, "Peripheral astigmatism in the human eye: experimental data and theoretical predictions," J. Opt. Soc. Am. **64**, 510–513 (1974).
29. D. D. R. Williams, P. Artal, R. Navarro, R. N. McMahon, and D. Brainard, "Off-axis optical quality and retinal sampling in the human eye," Vision Res. **36**, 1103–1114 (1996).

30. J. A. M. Jennings and W. N. Charman, "Off-axis image quality of the human eye," Vision Res. **21**, 445–455 (1981).
31. M. C. Dunne, G. P. Misson, E. K. White, and D. A. Barnes, "Peripheral astigmatic asymmetry and the angle alpha," Ophthalmic Physiol. Opt. **13**, 303–305 (1993).
32. Y. Z. Wang, L. N. Thibos, and A. Bradley, "Effects of refractive error on detection acuity and resolution acuity in peripheral vision," Invest. Ophthalmol. Visual Sci. **38**, 2134–2142 (1997).
33. T. Wertheim, "Über die indirekte Sehschärfe," Z. Psychol. Physiol. Sinnesorgane **7**, 172–187 (1894).
34. W. Smith, *Modern Optical Engineering* (McGraw-Hill, New York, 1966), p. 321.
35. C. R. Ferree, G. Rand, and C. Hardy, "Refraction for the peripheral field of vision," Arch. Ophthalmol. **5**, 717–731 (1931).
36. W. Hodos and J. T. Erichsen, "Lower field myopia in birds: an adaptation that keeps the ground in focus," Vision Res. **30**, 653–659 (1990).
37. F. W. Fitzke, B. P. Hayes, W. Hodos, A. L. Holden, and J. C. Low, "Refractive sectors in the visual field of the pigeon eye," J. Physiol. (London) **369**, 17–31 (1985).
38. F. Schaeffel, G. Hagel, J. Eikerman, and T. Collett, "Lower-field myopia and astigmatism in amphibians and chickens," J. Opt. Soc. Am. A **11**, 487–495 (1994).
39. J. Wallman, J. Winawer, X. Zhu, and T. W. Park, "Might myopic defocus prevent myopia?" in *Proceedings of the 8th International Conference on Myopia*, F. Thorn, D. Troilo, and J. Gwiazda, eds. (Published by editors, Boston, Mass., 2000), pp. 138–142.
40. F. Rempt, J. Hooger-Heide, and W. P. H. Hoogenboom, "Peripheral retinoscopy and the skiagram," Opththalmologica **165**, 1–10 (1971).
41. E. L. Smith, J. Huang, and L. F. Huang, "Cylindrical spectacle lenses alter emmetropization and produce astigmatism in young monkeys," in *Myopia Updates. Proceedings of the 6th International Conference on Myopia*, T. Tokoro, ed. (Springer, Berlin, 1998), pp. 336–343.
42. R. C. McLean and J. Wallman, "Despite severe imposed astigmatic blur, chicks compensate for spectacle lenses," Invest. Ophthalmol. Visual Sci. Suppl. **38**, #2521 (ARVO abstract 1997).
43. K. Schmid and C. F. Wildsoet, "Natural and imposed astigmatism and their relation to emmetropization in the chick," Exp. Eye Res. **64**, 837–847 (1997).
44. A. Seidemann, A. Guirao, P. Artal, and F. Schaeffel, "Peripheral sphere and astigmatism measured by infrared photoretinoscopy and by double pass point spread," in *Vision Science and Its Applications*, Vol. 1 of 1999 OSA Technical Digest Series (Optical Society of America, Washington, D.C., 1999), pp. 224–227.